

SANDIA REPORT

SAND88-8691
Unlimited Release
Printed April 1988

DTIC FILE CODE

①

DTIC FILE CODE

AD-A197 515

HgI₂ Near-bandgap Photoluminescence Structure and Its Relationship to Nuclear Detector Quality

(Published in Journal of Applied Physics)

D. Wong, T. E. Schlesinger, R. B. James, C. Ortale, L. van den Berg, W. F. Schnepfle

Prepared by
Sandia National Laboratories
Albuquerque, New Mexico 87185 and Livermore, California 94550
for the United States Department of Energy
under Contract DE-AC04-76DP00789

DTIC
SELECTED
JUL 9 9 1988

SAND88-8691
Unlimited Release
Printed April 1988

HgI₂ NEAR-BANDGAP PHOTOLUMINESCENCE STRUCTURE AND ITS RELATIONSHIP TO NUCLEAR DETECTOR QUALITY

D. Wong, T. E. Schlesinger
Department of Electrical and Computer Engineering
Carnegie Mellon University, Pittsburgh, PA 15213

R. B. James
Theoretical Division
Sandia National Laboratories
Livermore, CA 94550

C. Ortale, L. van den Berg, and W. F. Schnepfle
EG&G Energy Measurements, Inc.
Goleta, CA 93116



| | |
|--------------------|-------------------------------------|
| Accession For | |
| NTIS CR&I | <input checked="" type="checkbox"/> |
| DTIC TAB | <input type="checkbox"/> |
| Unannounced | <input type="checkbox"/> |
| Justification | |
| By _____ | |
| Distribution/ | |
| Availability Codes | |
| Dist | Avail and/or Special |
| A-1 | |

Abstract

The low-temperature photoluminescence spectra of several mercuric iodide detectors and off-stoichiometric bulk material have been characterized. Phonon energies have been determined with Raman spectroscopy over a range of temperatures. In earlier work some of the near-bandgap photoluminescence features were identified as phonon replicas. After careful examination of Raman and photoluminescence data, we find that one or perhaps more of these features are probably due to shallow electronic levels related to native defects. Suggestions as to the relationship between photoluminescence peaks and detector quality are made.

Introduction

→Mercuric iodide is of interest because it is a high-Z material suitable for applications in nuclear radiation detection. It has an advantage over the more commonly used silicon and germanium detectors in that, with its larger bandgap, it can be operated at room temperature. However, several problems exist in using it for fabricating nuclear detectors, an outstanding one being process control during fabrication.

part 2
The quality of the material and the detectors shows wide variation. Different detectors made out of material from the same crystal can perform very differently [1]. As yet there are many unanswered questions as to the electronic entities which cause a detector to perform poorly. Work has been done using thermally stimulated current (TSC) techniques to identify deep traps [2], and attempts have been made to relate traps to process conditions and stoichiometry [3].

Wu et al. [4] and Merz et al. [5] performed low-temperature photoluminescence measurements in an attempt to establish a connection between the stoichiometry and impurity content of the material and its photoluminescence spectrum. They suggested relationships between broad photoluminescence peaks of energies substantially lower than the band gap and impurity content and non-stoichiometry, and also observed detailed structure near the band-edge energy. Following up earlier work by Novikov and Pimonenko [6], they reasserted the interpretation that the near-bandgap structure is composed entirely of four exciton lines and their phonon replicas.

Several Raman studies have been done on mercuric iodide for reasons not related to its applications in radiation detection. Understanding of the well known phase

transition which it undergoes at 400 K has been the motivation for a number of Raman scattering measurements on the material. Hence, the phonon energies of mercuric iodide at room temperature and above are well documented. Two of the four most commonly quoted Raman (optically) active phonon modes in red mercuric iodide [7] roughly correspond to the phonon energies quoted in the photoluminescence work mentioned above.

Most of the work done to date on characterising traps and defects in mercuric iodide has been with HgI_2 bulk crystals. In the present study, we use photoluminescence and Raman scattering at low temperatures (ranging from 4.2 K to 78 K) to study actual detectors of varied quality and compare the results with specimens of bulk material we have reason to believe to be non-stoichiometric. In this way we have attempted to identify shallow levels in the material which are introduced in the detector processing and have some effect on detector performance.

Experimental method

Measurements were made on two categories of specimens : fully processed detectors and bulk material. The detectors were made from slices cut from bulk crystals which were then etched and polished. Palladium contacts were evaporated onto both sides of each slice, and the devices were then assessed in terms of their response to 662-keV radiation from a ^{137}Cs source, graded in quality in terms of energy resolution and peak to valley ratio and classified as either A, B, C or D type, with the A group being detectors of highest quality. A fuller description of the crystal growth, fabrication, testing and classification of the detectors used in the experiments is described in ref. [1].

One bulk material sample studied was a specimen of poor quality material, this being material that produced detectors that were all either grade C or D. We also studied HgI_2 crystals that were grown off stoichiometry. Iodine rich or iodine deficient specimens were obtained by using starting material in the crystal growth process with either an iodine rich or poor content. The colour of the material that condenses on the side walls of the ampoule used in the crystal growth and the colour of the gas within this ampoule are used as qualitative measures of the iodine content; that is, a deeper hue of reddish-pink indicates more iodine in the HgI_2 crystals. (In a separate experiment we added excess iodine to the starting material and verified that there was an increased reddish-pink colour of the gas and condensed material in the ampoule.) The iodine rich and iodine poor specimens selected for this work showed the greatest and least reddish-pink hue among a group of many different HgI_2 crystals. Although the bulk stoichiometry is different for our iodine rich and poor samples, we would like to point out that there is no clear evidence that surface and bulk stoichiometry is the same, especially after the processing steps required for detector fabrication [1,2].

The optical excitation source used for the photoluminescence measurements was an argon laser operating at 5145 angstroms. The photoluminescence was analysed with a Spex 1404 double pass spectrometer with entrance and exit slit widths set at 1mm. This corresponds to a resolution of about 4 angstroms in the wavelength range of interest. A cooled (77 K) S-1 response photomultiplier was used as a detector. The laser light excitation was chopped at 750 Hz, and the photomultiplier output was coupled via a Keithley 427 current amplifier to an EG&G 5207 lock-in amplifier.

The photoluminescence was collected from the front surfaces of the detector

specimens. In nuclear radiation detection, the radiation to be sensed is absorbed throughout the entire detector, but charge collection is at the front and back surfaces.

Raman spectroscopy was used to determine the optical phonon energies. The Raman measurements were carried out using an experimental set up essentially identical to that described above for the photoluminescence measurements, but with laser excitation from a dye laser operating at a wavelength of 8300 angstroms.

Experimental results and discussion

a) Raman measurements

We have used Raman scattering to measure the energies of three optical phonons corresponding to what have been called longitudinal phonons LO_1 , LO_2 and LO_3 in the literature [8]. To determine the phonon energy values applicable to our particular samples in conditions similar to the experimental conditions under which the photoluminescence spectra were taken, a set of Raman measurements were made on a bulk specimen at 4.2 K, 30 K and 78 K. The LO_3 phonon was observed at an energy of 14.2 meV with a spread of ± 0.03 meV in energy value over three different runs. The LO_2 phonon was found to have an energy of 3.9 meV at 4.2 and 30 K. Room temperature measurements showed the LO_1 phonon to have an energy of 2.2 meV. The discussion which follows centres around the LO_3 phonon, and we will take the relevant energy for this phonon to be 14.2 meV with an error margin of ± 0.05 meV. This energy value is independent of temperature for the temperature range over which the photoluminescence experiments were conducted (4.2 K to 30 K).

Previous Raman studies at room temperature reported energy values for these

three phonons ranging from 14.1 meV to 14.4 meV (LO_3); 3.6 meV to 4.0 meV (LO_2); and 2.1 meV to 2.6 meV (LO_1) [7,9,10]. The LO_1 phonon and LO_3 phonons correspond respectively to the TO and LO phonons referred to in [5] and [6].

b) The photoluminescence spectra

Figs. 1a and 1b show photoluminescence spectra taken at 4.2 K for two detector and three bulk material specimens. All the spectra have similar features - a main peak at about 5320 angstroms with a shoulder on its shorter wavelength side and a series of smaller peaks immediately to its longer wavelength side. These comprise what Merz et al. [5] designate as Band 1. Following the same notation, Band 2 can be seen at about 5590 angstroms. Band 3, a broad peak at 6200 angstroms, is not shown in these spectra but was observed to be present in the spectra of many of the specimens, though at very low intensities compared to Band 1. Typically Band 3 was reduced by at least one and a half orders of magnitude compared to Band 1 at 77 K, and it was even less apparent at 4.2 K. Merz et al. suggested that this band is impurity related, and if this is the case, the specimens used for the measurements reported in this paper are relatively free of these impurities.

The bandgap of mercuric iodide at 4.2 K has been optically determined to be 5230 angstroms (2.3707 eV) [8]. Fig. 2 is a spectrum showing the near band edge structure for one of the detector specimens. In the figure we define a new notation, which is introduced to avoid the referencing of peaks in terms of phonon replicas, as is employed by both Merz et al. [5] and Novikov and Pimonenko [6]. The average peak positions at 4.2 K were extracted from sixteen spectra taken from five different detector and bulk material specimens and these are listed in table 1. It can be seen from table 1 that each

of our peaks P1 through P9 correspond to features reported in references [5] and [6].

c) A closer examination of the near-bandgap photoluminescence

The spectra of fig. 1a, and others taken in the course of these experiments, indicate that one difference between A ('good') detectors and D ('poor') detectors is that the peaks P5, P6, P8 and (occasionally) P9 tend to be more pronounced in the D detectors, relative to the P3 intensity (these peaks having up to an order of magnitude greater relative intensity in D detectors). The 'bad' material is similar to the D detectors in this respect.

Fig. 1b shows that the iodine deficient specimen is also similar to D detectors in having large P5, P6 and P8 peaks, and that the iodine rich material shows large P5, P6, P8 and P9 peaks. The iodine deficient and iodine rich bulk specimens also show other enhanced peaks between P9 and Band 2 which may perhaps be related to non-stoichiometry. This paper will, however, focus primarily on the P5, P6 and P8 peaks.

We have already reported that in 78 K luminescence spectra, a shoulder at approximately 5424 angstroms is indicative of detector quality, this feature being prominent in poor detectors [1]. Fig. 3 shows a set of photoluminescence spectra taken at different temperatures for a D detector, clearly indicating that the shoulder to the lower energy side of the main peak at 78 K corresponds to the P8 peak in the 4.2 K spectra.

Novikov and Pimonenko [6] identify the peaks we label P6 and P8 as $1LO_3$ and $2LO_3$ replicas of P3 respectively, and they identify P5 as a $1LO_3$ replica of P1. Merz et al. [5] also subscribe to this idea. It seems unlikely however that phonon replicas would vary widely in magnitude relative to their no-phonon lines from specimen to specimen

and be more pronounced in poor quality material.

Table 2 lists peak separation values as determined in our experiments and also as extracted from data reported in [5] and [6]. Data from the present work listed in table 2 was obtained by taking averages of the separations of peaks as they appeared in nine different photoluminescence spectra. The P3 - P8 separation appears too small to be accounted for as a $2LO_3$ phonon replica : Our data shows this separation to be 27.3 meV with a σ_{n-1} margin of 0.1 meV. From the Raman data, however, the $2LO_3$ phonon energy equals 28.4 meV with an error margin of 0.1 meV. There is no similar difficulty with the P3 - P6 separation that we have measured. This argument is based on the assumption that the peak P3 has its origin in some direct electronic transition -- Raman measurements yield phonon energies of zone centre phonons. Mercuric iodide has been identified as an indirect bangap material ([11],[12]). Nevertheless, there are grounds for identifying P3 as corresponding to a direct transition and this will be discussed in subsection (2).

To confirm the supposition that P8 is not a phonon replica of P3, a number of temperature varied photoluminescence spectra were taken. Given that the Raman measurements verified the fact that phonon energies are independent of temperature over the range 4.2 K to 78 K, it follows that the separation between a no-phonon line and its phonon replica will remain constant as the temperature is varied between these limits. Care was taken to choose a position on each specimen which gave a spectrum in which the main peak was unequivocally P3 : Novikov and Pimonenko's λ_2 peak [6]. These authors point out that with some specimens the λ_2 peak was predominant and in others the peak they designate as λ_x (P2), situated at some four angstroms to the longer

wavelength side, was the principal peak. Spectra were taken at different temperatures without changing the specimen position or optical alignment. Data was obtained in the wavelength domain (the spectrometer has a constant wavelength window width) and then mapped numerically onto the energy domain. The main peak energy for each spectrum was subtracted to give sets of graphs defining peak positions in terms of energy distance from the main peak P3. Examples of these graphs are shown in figs. 4a and 4b which show the results for an A detector and for the iodine deficient material respectively. It can be seen from these graphs that in both cases the P3 - P8 separation does vary with temperature.

The spectra in figs. 4a and 4b show that the position of P6 is more or less constant with respect to P3 for the different measurement temperatures, as far as can be ascertained given the limitation that at higher temperatures P6 is a small peak on a falling slope.

The distortion of the shape of P8 with increased temperature, as can be seen clearly in fig. 4a, warrants consideration. It could be that the nature of the transition which is the origin of P8 is such that it is asymmetric in wavelength at raised temperatures. Another possibility is that P8 is in fact a composite peak and that one of its components strengthens with temperature. This to some extent compromises the observation that P8 shifts with respect to P3 with rising temperature. Nevertheless, it still remains true that there is some element of P8 which is not merely phonon replication of P3 and which is indicative of material quality.

The spectra of figs. 4a, 4b and other sets of spectra taken in the course of the experiments showed that while P8 strengthened monotonically with increasing

temperature, P3 decreased in magnitude with temperature. The exciton-to-defect binding energy is of the order of 10 meV [6], far larger than thermal energy kT in the range 4.2 to 30 K. Hence, it would be expected that the degree of phonon coupling would be essentially independent of temperature over this range, and that a phonon replica would have a more or less constant magnitude relative to its no-phonon line for different temperatures. This provides further evidence that there is at least some component of P8 which is not a phonon replica of P3.

d) The question of whether P3 corresponds to a direct transition

Chester and Coleman [11] performed electroabsorption measurements on mercuric iodide to find that the field dependence of the major electroabsorption peak at 88 K and 300 K followed a power law corresponding closely to the theoretical formula for indirect transitions. Yee et al. [12] derived the band structure theoretically using the pseudopotential technique and also arrived at the conclusion that the bandgap of HgI_2 is indirect.

On the other hand the 4.2 K absorption spectrum reported by Novikov and Pimonenko [6] is strongly indicative of direct bandgap material. Clear peaks corresponding to the ground state and first two excited states in the free exciton series are resolved. For indirect transitions it would be expected that the exciton states would give rise to a continuous absorption since phonons can be found to give transitions for all crystal momentum values [13]. It would thus appear that the free exciton peaks observed in Novikov and Pimonenko's absorption and photoluminescence spectra correspond to direct transitions. The separation between P3 and the direct ground state free exciton in their work corresponds to an exciton-to-defect binding energy of 10.7

meV. Novikov and Pimonenko plotted the intensity of the P3 luminescence against temperature to arrive at a P3 exciton-to-defect binding energy close to this value [14] (12 meV). This implies that P3 corresponds to a direct transition.

In the present work it was found that P3 and sometimes P2 dominated the photoluminescence spectra at 4.2 K, being more than an order of magnitude stronger than the other peaks in most spectra. P3 corresponds to a transition involving an exciton bound to a defect with an exciton-to-defect binding energy (E_{Bx}) : Exciton binding energy (E_x) ratio of about 0.4 (computed from values given in [6,14]). Dean [15] suggested on empirical grounds that a measure of the strength of phonon coupling for any given bound exciton in an indirect material is given by E_{Bx}/E_x . Weakly bound excitons (small E_{Bx}/E_x) demonstrate strong phonon coupling. An example of a "weakly bound" exciton in an indirect bandgap material is the nitrogen-exciton line in SiC with an E_{Bx}/E_x ratio of about 0.74 (computed from data in [16]) which has phonon replicas of magnitudes slightly greater than the no-phonon line in 6 K photoluminescence spectra [17]. The absence of similarly strong phonon replication of P3 in mercuric iodide further implies that P3 corresponds to a direct transition.

Summary

We have obtained data which indicates that phonon energies are temperature independent at low temperatures, and have suggested suitable values and error margins for these phonon energies over the temperature range 4.2 K to 30 K. Our data, coupled with other observations, indicates that P8 is not a phonon replica of P3, contrary to what has been reported in previous work.

The fact that P5 and P8 are enhanced in both iodine deficient and iodine rich

material suggests that they may be related to material non-stoichiometry. While we have not succeeded in disproving the idea that P6 is a phonon replica of P3, we have shown that this conjecture has some shortcomings. Hence, the possibility that P6 may be related to non-stoichiometry in a manner similar to P5 and P8 should also be considered.

Referring back to figs. 1a and 1b, the qualitative similarities in the spectra of the iodine deficient material, the iodine rich material, and the D detector (poor quality) spectra suggest that crystal growth which results in either bulk or local non-stoichiometry is unlikely to produce material which can be made into high quality detectors. It would in fact appear that, whatever the origin of peaks P5, P6 and P8, any process which results in material which has a photoluminescence response that shows any or all of these peaks strongly is to be avoided. In [1] it was reported that detectors made by evaporation of palladium contacts onto slices from the same crystal which might accordingly be expected to be similar in quality did in fact show a very wide difference in performance. Auger spectroscopy has shown that stoichiometry changes occur when HgI_2 is exposed to vacuum [18]. It would thus seem that the steps involved in laying down palladium contacts for the fabrication of detectors from bulk material may in some cases introduce local/surface non-stoichiometry which can have an adverse effect on detector performance.

Acknowledgments

We would like to acknowledge D. K. Ottesen, R. H. Stulen, T. E. Felter, Larry Franks, M. I. Baskes and G. Gentry for many useful discussions. One of us (T.E.S.) would like to acknowledge the support of IBM through a Faculty Development Award.

References

1. R. B. James, D. K. Ottesen, D. Wong, T.E. Schlesinger, W. F. Schneppe, C. Ortale and L. van den Berg, to be published.
2. T. Mohammed-Brahim, A. Friant and J. Mellet, *Phys. Stat. Sol. (a)* **79**, 71 (1983).
3. R. C. Whited and L. van den Berg, *IEEE Trans. Nucl. Sci.* **24**, 165 (1977).
4. Z. L. Wu, J. L. Merz, L. van den Berg and W. F. Schneppe, *J. Luminescence* **24/25**, 197 (1981).
5. J. L. Merz, Z. L. Wu, L. van den Berg and W. F. Schneppe, *Nucl. Instr. and Meth.* **213**, 51 (1983).
6. B. V. Novikov and M. M. Pimonenko, *Sov. Phys. Semicond.* **4**, 1785 (1971).
7. A. J. Melveger, R. K. Khanna, B. R. Guscott and E. R. Lippincott, *Inorg. Chem.* **7**, 1630 (1968).
8. T. Goto and Y. Nishina, *Solid State Commun.* **15**, 123 (1978).
9. D. M. Adams and M. A. Hooper, *Aust. J. Chem.* **24**, 885 (1971).

10. Shinichi Nakashima, Hiroaki Mishima, and Akiyoshi Mitsuishi, *J. Raman Spectroscopy* **1**, 325 (1973).
11. M. Chester and C. C. Coleman, *J. Phys. Chem. Solids* **32**, 223 (1971).
12. J. H. Yee, J. W. Sherohman, and G. A. Armantrout, *IEEE Trans. Nucl. Sc. NS-23*, 117 (1976).
13. R. J. Elliott, *Phys. Rev.* **108**, 1384 (1957).
14. B. V. Novikov and M. M. Pimonenko, *Sov. Phys. Semicond.* **4**, 1785 (1971).
15. P. J. Dean, *Phys. Rev.* **157**, 655 (1967).
16. D. S. Nedzvetskii, B. V. Novikov, N. K. Prokofeva, and M. B. Reifman, *Sov. Phys. Semicond.* **2**, 914 (1969).
17. W. J. Choyke, D. R. Hamilton, and Lyle Patrick, *Phys. Rev.* **133**, A1163 (1964).
18. T. E. Felter, R. H. Stulen, W. F. Schnepple, C. Ortale, and L. van den Berg, to be published.

| This work (4.2 K) | | | Ref. [6] (4.2 K) | | Ref. [5] (1.6 K) | |
|-------------------|-------------------|----------------|------------------|-------------------|------------------|-------------------|
| Peak | Wavelength (Å) | | Peak | Wavelength (Å) | Peak | Wavelength (Å) |
| | Mean | σ_{n-1} | | | | |
| P1 | 5311.0 | 0.9 | λ_1 | 5309.5 | 1A | 5312.4 |
| P2 | 5318.3 | --- | λ_x | 5316.9 | 1B | 5319.7 |
| P3 | 5322.5 | 0.5 | λ_2 | 5321.6 | 1C | 5322.9 |
| P4 | 5329.4 | 0.4 | λ_0 -LO | 5328.5 | 1A*-LO | 5328.3 |
| P5 | 5341.2 | 0.7 | --- | --- | 1A-LO | 5339.4 |
| P5' | 5344.0 | --- | λ_1 -LO | 5344.2 | 1A-L0 | 5343.0 |
| P6 | 5355.1 | 0.9 | λ_2 -LO | 5354.8 | 1C-LO | 5355.5 |
| P7 | 5369.9 | 1.1 | λ_1 -2LO | 5370.8 | 1A-2LO | 5369.7 |
| P8 | 5385.2 | 0.7 | λ_2 -2LO | 5383.4 | 1C-2LO | 5386.2 |
| P9 | 5394.5 | 0.6 | λ_0 -3LO | 5394.5 | 1A*-3LO | 5394.4 |

Table I : Photoluminescence peak positions and standard deviations of average peak positions. P2 position estimated from 2 spectra. P5' position based on single spectrum. P1 position as read without correction for P1 lying on a steep slope. The true P1 position is about 1 angstrom less than its tabulated value.

| This work (4.2 K) | | | Ref [6] (4.2 K) | | Ref [5] (1.6 K) | | This work | |
|-------------------|--------------|----------------|-----------------------------|--------------|-----------------|--------------|-----------|--------------|
| Peaks | Energy (meV) | | Peaks | Energy (meV) | Peaks | Energy (meV) | Phonon(s) | Energy (meV) |
| | Mean | σ_{n-1} | | | | | | |
| P3-P6 | 14.3 | 0.1 | $\lambda_2-(\lambda_2-LO)$ | 14.4 | 1C-(1C-LO) | 14.2 | LO_3 | 14.2 |
| P3-P8 | 27.3 | 0.1 | $\lambda_2-(\lambda_2-2LO)$ | 26.7 | 1C-(1C-2LO) | 27.4 | $2LO_3$ | 28.4 |

Table II : Photoluminescence peak separations and standard deviations of peak separations.

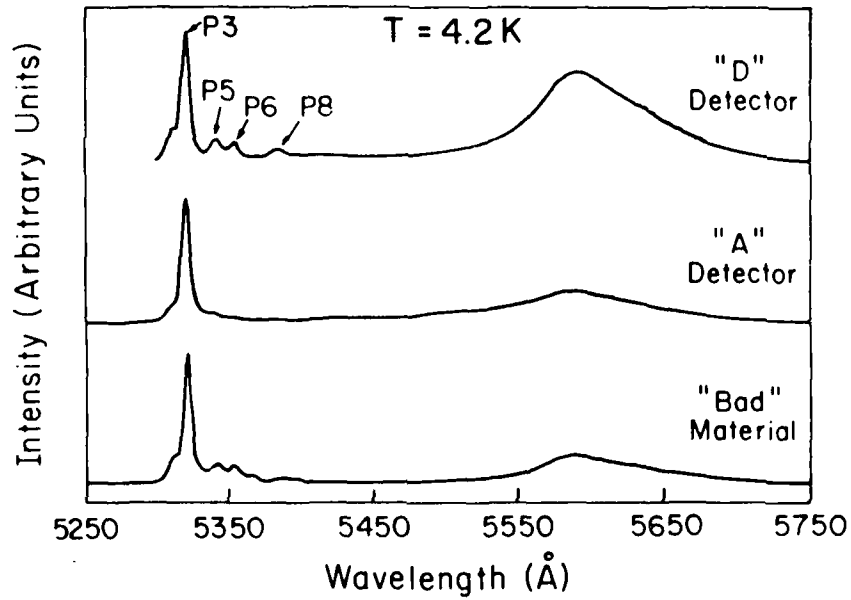


Figure 1a. Photoluminescence spectra of detectors and detector material

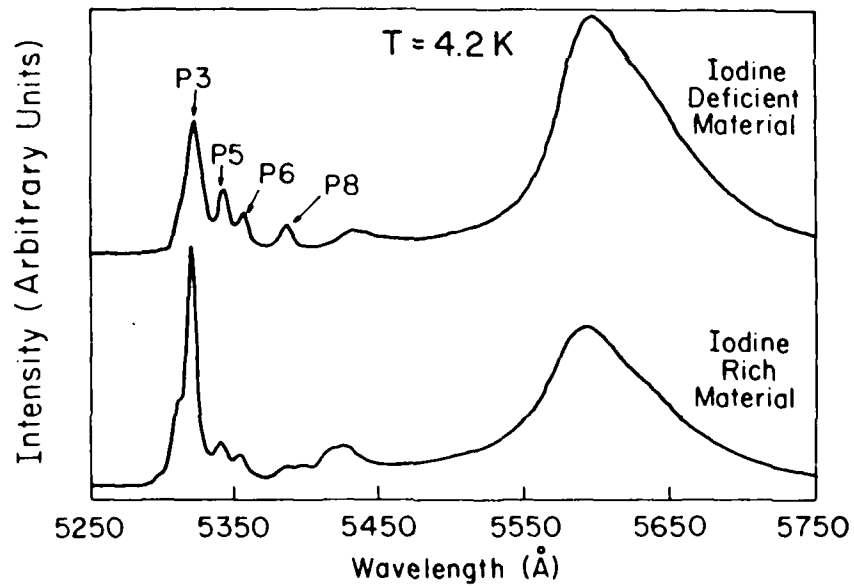


Figure 1b. Photoluminescence spectra of off-stoichiometric bulk material.

The peaks P5, P6, and P8 appear more prominently in the spectra of the D detector, "bad" material and off stoichiometric material than they do in the A detector spectrum.

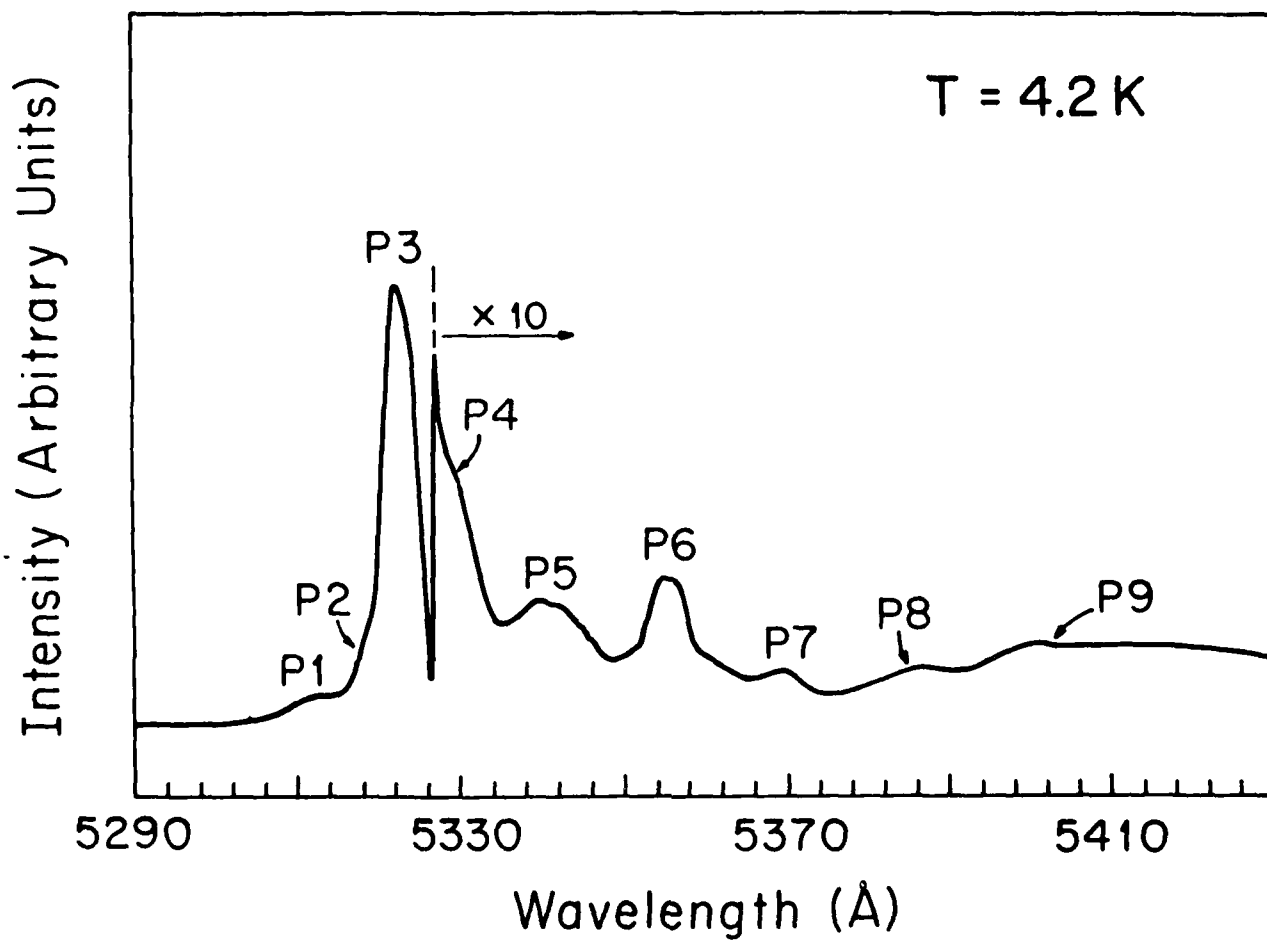


Figure 2. Peak labelling for a B detector photoluminescence spectrum taken at 4.2 K.

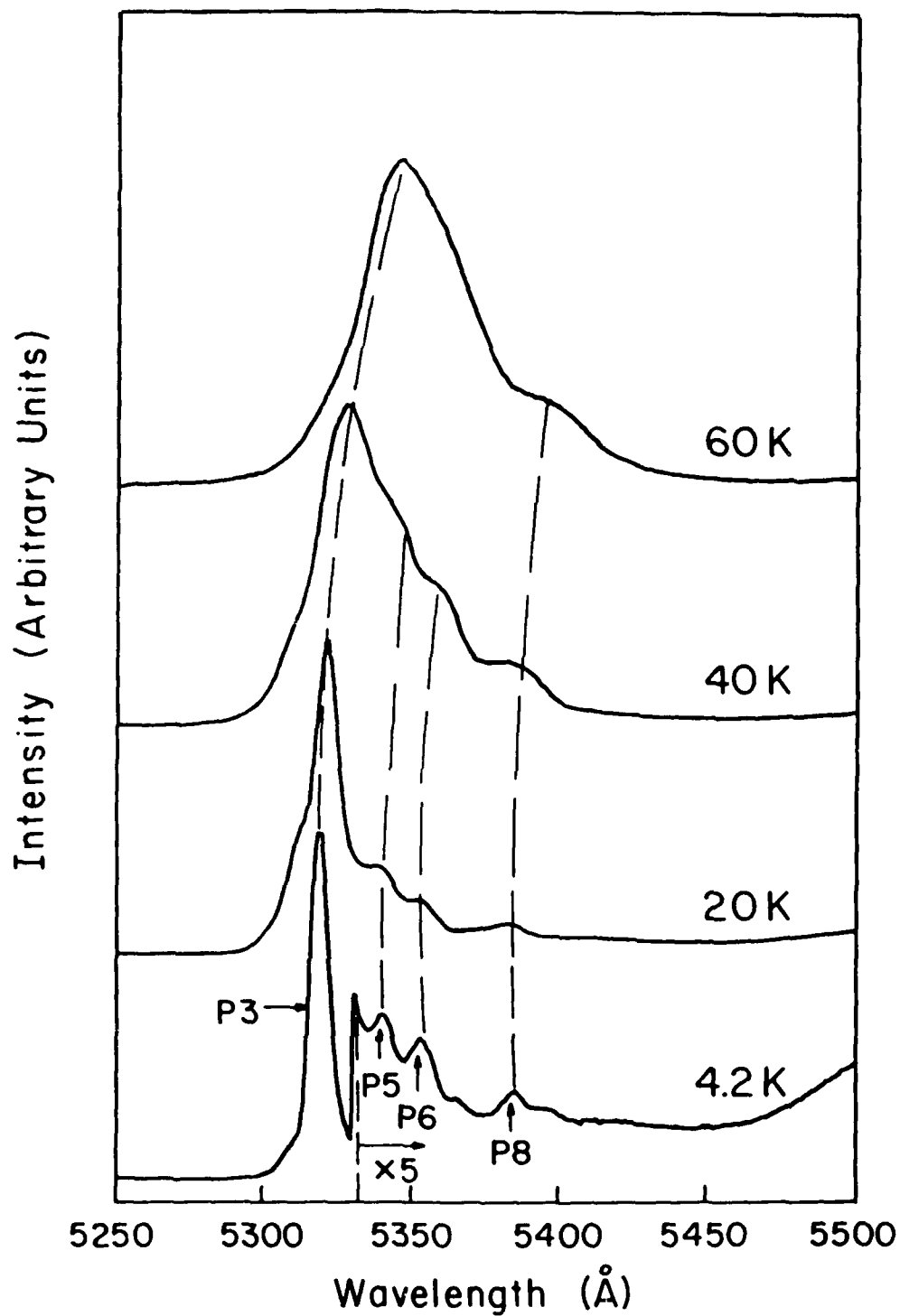


Figure 3. Photoluminescence spectra at different temperatures for a D detector. With rising temperature the peaks P5 and P6 merge with the main peak P3 to broaden it. Peak P8 forms a shoulder which also appears in liquid nitrogen 77 K spectra.

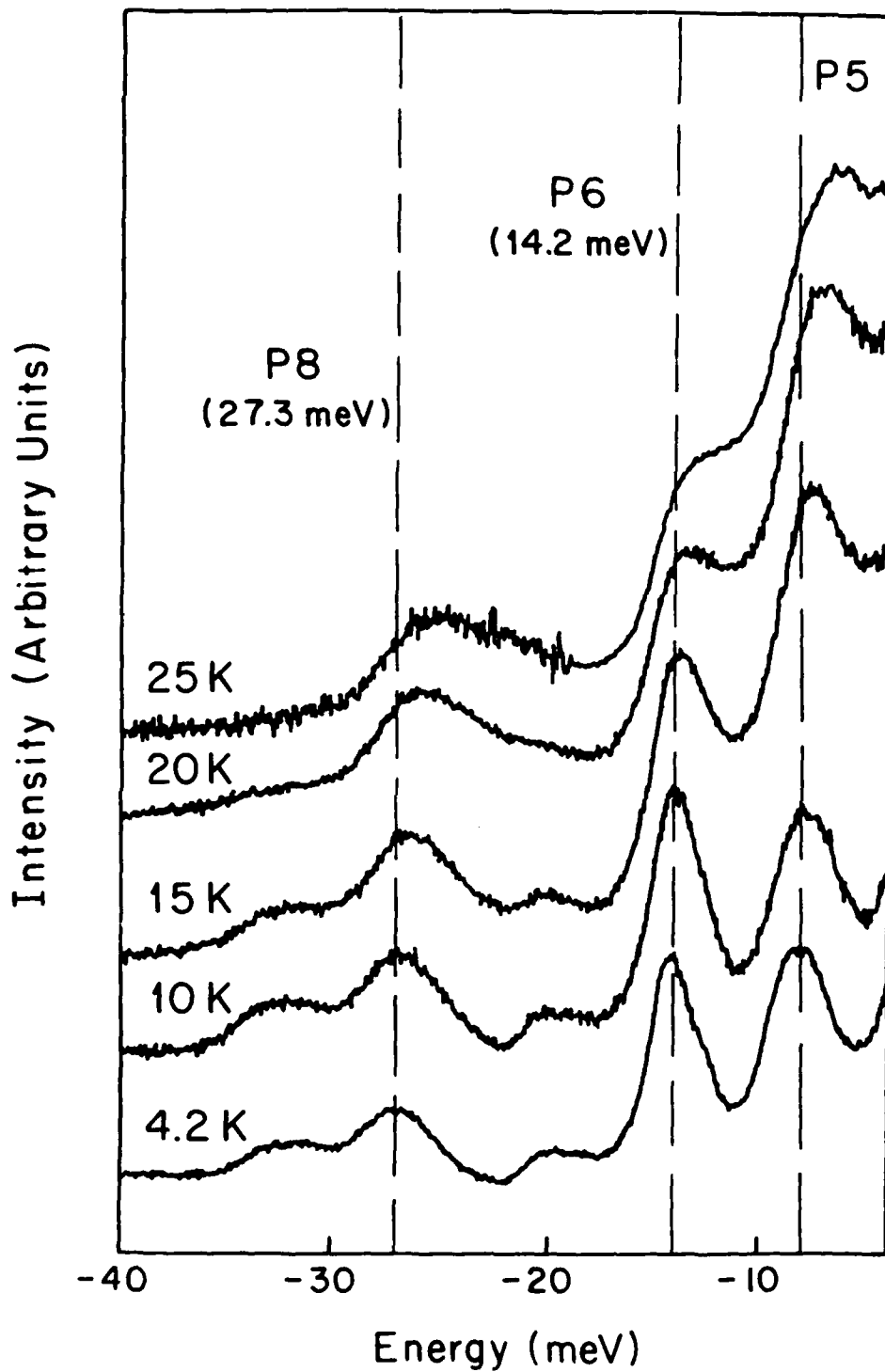


Figure 4a. Photoluminescence spectra at different temperatures for an A detector, with peak P3 taken as the zero reference.

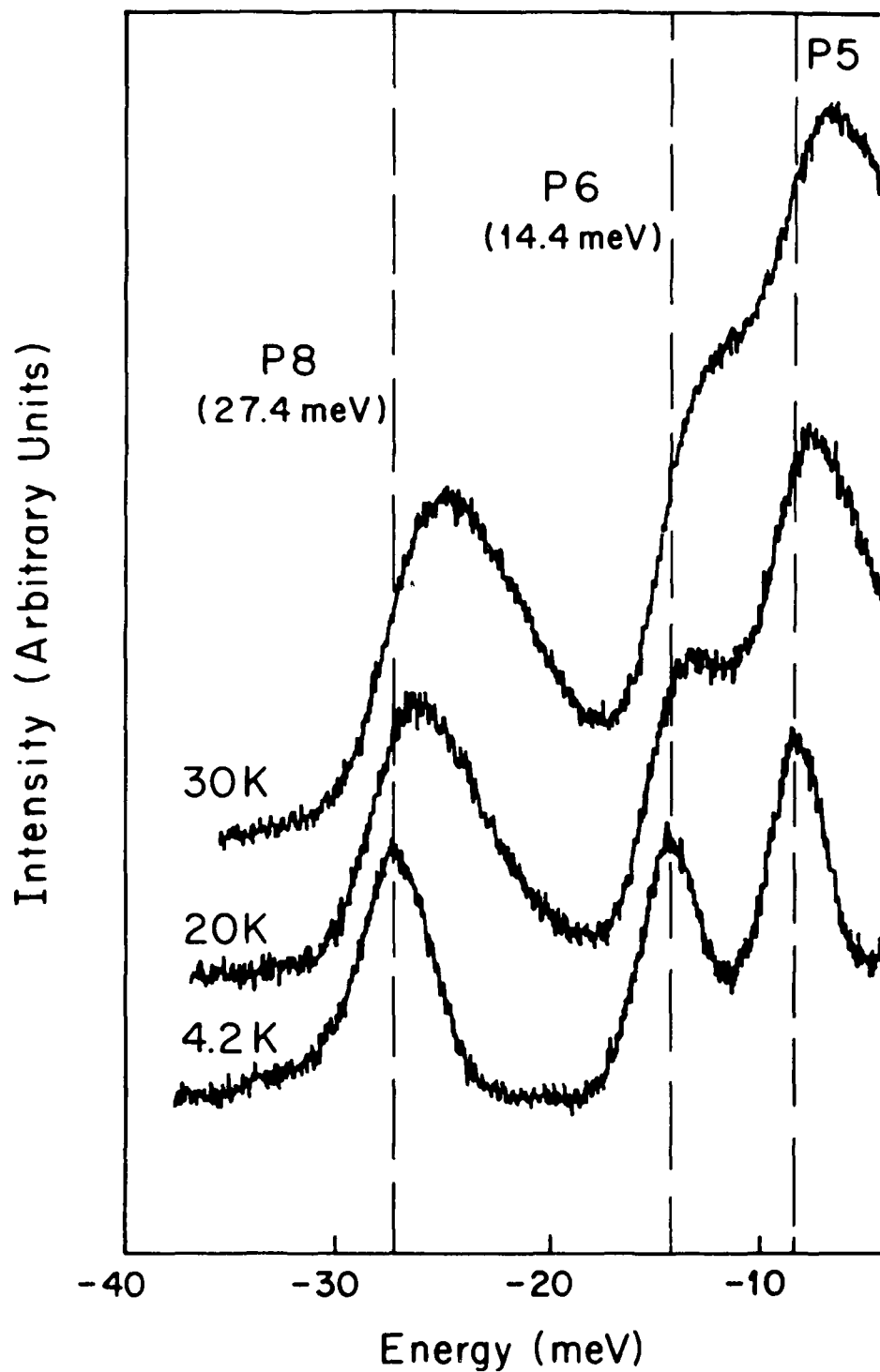


Figure 4b. Photoluminescence spectra at different temperatures for the iodine deficient material, with peak P3 taken as the zero reference.

UNLIMITED RELEASE
INITIAL DISTRIBUTION

Abteilung C1
Hahn-Meitner Institut
Attn: J. R. Schneider
Glienickerstr. 100
D-1000 Berlin 39
F. R. G.

Albert-Ludwigs-Universität
Kristallographisches Inst.
Attn: M. Grün
Helberstr. 25
7800 Freiburg
F. R. G.

Albert-Ludwigs-Universität
Kristallographisches Inst.
Attn: H. Marquardt
Helberstr. 25
7800 Freiburg
F. R. G.

Albert-Ludwigs-Universität
Kristallographisches Inst.
Attn: K. Wacker
Helberstr. 25
7800 Freiburg
F. R. G.

AFIF
ETH Hönggerberg
Attn: S. Blunier
8093 Zürich
Switzerland

AFIF
ETH Hönggerberg
Attn: H. Zogg
8093 Zürich
Switzerland

Aristot. Univ. Thessaloniki
Physics Department
Attn: E. K. Polychroniadis
54006 Thessaloniki
Greece

Carnegie Mellon University (5)
Dept. of Elec. & Computer Eng.
Attn: T. E. Schlesinger
Pittsburgh, PA 15213

Contraves
Attn: H. Stanna
Schaffhauserstr. 580
8052 Zürich
Switzerland

EG&G Energy Measurements Inc.
Santa Barbara Operations
Attn: A. Beyerle
130 Robin Hill Road
Goleta, CA 93117

EG&G Energy Measurements Inc.
Santa Barbara Operations
Attn: A. Y. Cheng
130 Robin Hill Road
Goleta, CA 93117

EG&G Energy Measurements Inc.
Santa Barbara Operations
Attn: L. A. Franks
130 Robin Hill Road
Goleta, CA 93117

EG&G Energy Measurements Inc.
Santa Barbara Operations
Attn: V. M. Gerrish
130 Robin Hill Road
Goleta, CA 93117

EG&G Energy Measurements Inc.
Santa Barbara Operations
Attn: H. A. Lamonds
130 Robin Hill Road
Goleta, CA 93117

EG&G Energy Measurements Inc.
Santa Barbara Operations
Attn: J. M. Markakis
130 Robin Hill Road
Goleta, CA 93117

EG&G Energy Measurements Inc.
Santa Barbara Operations
Attn: C. Ortale
130 Robin Hill Road
Goleta, CA 93117

EG&G Energy Measurements Inc.
Santa Barbara Operations
Attn: B. E. Patt
130 Robin Hill Road
Goleta, CA 93117

EG&G Energy Measurements Inc.
Santa Barbara Operations
Attn: M. Schieber
130 Robin Hill Road
Goleta, CA 93117

EG&G Energy Measurements Inc.
Santa Barbara Operations
Attn: W. F. Schneppe
130 Robin Hill Road
Goleta, CA 93117

EG&G Energy Measurements Inc.
Santa Barbara Operations
Attn: N. Skinner
130 Robin Hill Road
Goleta, CA 93117

EG&G Energy Measurements Inc.
Santa Barbara Operations
Attn: L. van den Berg
130 Robin Hill Road
Goleta, CA 93117

ESA
Microgravity Office
Attn: G. Seibert, Prog. Mgr.
8-10, Rue Mario-Nikis
75738 Paris, Cedex 15
France

ESA
Microgravity Office
Attn: H. Walter, Senior Scientist
8-10, Rue Mario-Nikis
75738 Paris, Cedex 15
France

Fachbereich Physik
Universität Siegen
Attn: H.-J. Besch
Adolf-Reichweinstr.
5900 Siegen 21
F. R. G.

Ferroperm Ltd.
Electronic Components
Attn: P. Lindhardt
Stubbeled 7, Trorod
2950 Vedbaek
Denmark

Fisk University
Dept. of Physics
Attn: E. Silberman
Nashville, TN 37203

Global Geochemistry Corp.
Attn: S. Steinberg
6919 Eton Avenue
Canoga Park, CA 91303

The Graduate School, Nagatsuta
Tokyo Inst. Technology
Attn: T. Kobayashi
Midori-ku, Jokohama 227
Japan

Hebrew University Jerusalem
School of Applied Sci. Technol.
Attn: A. Burger
Jerusalem
Israel

Inst. Angewandte Physik
Universität Karlsruhe
Attn: U. Birkholz
Kaisestr. 12
D-7500 Karlsruhe
F. R. G.

Inst. Mittelenergiephysik
ETH Hönggerberg
Attn: J. Lang
8093 Zürich
Switzerland

IRDI
Dept. Electron. Instr. Nucl.
Attn: A. Friant
C.E.N. Saclay
91191 Gif-sur Yvette, Cedex
France

IRDI
Dept. Electron. Instr. Nucl.
Attn: J. Mellet
C.E.N. Saclay
91191 Gif-sur Yvette, Cedex
France

Institut für Physik
Universität Basel
Attn: I. Zschokke-Gränacher
Klingerbergstr. 82
4056 Basel
Switzerland

Inst. TESRE/CNR
Attn: G. Di Cocco
Via de Castagnoli 1
40126 Bologna
Italy

Inst. TESRE/CNR
Attn: W. Dusi
Via de Castagnoli 1
40126 Bologna
Italy

Inst. TESRE/CNR
Attn: C. Labanti
Via de Castagnoli 1
40126 Bologna
Italy

Instrum. Appl. Phys. Div.
Harwell
Attn: D. Tottendell
Oxfordshire OX11 0RA
England

Jap. Atomic Energy Res. Inst.
Attn: E. Sakai
Tokaimura Nakagun
Ibarakiken 319-11
Japan

Jet Propulsion Laboratory
California Inst. of Technology
Attn: J. G. Bradley
4800 Oak Grove Drive
Pasadena, Ca 92209

Jet Propulsion Laboratory
California Inst. of Technology
Attn: J. M. Conley
4800 Oak Grove Drive
Pasadena, Ca 92209

Jet Propulsion Laboratory
California Inst. of Technology
Attn: P. L. Schlichta
4800 Oak Grove Drive, 11-116
Pasadena, Ca 91109

Kristal-Mater. Labor.
Fak. Physik, Univ. Karlsruhe
Attn: G. Müller-Vogt
Kaiserstr. 12
7500 Karlsruhe 1
F. R. G.

Lab. Chimie Minerale 1
U.E.R. Sciences Exactes Nat.
Attn: J. Omaly
B. P. 45
63170 Aubière
France

Lab. Mineral-Cristallogr.
Attn: S. Léon-Gits
Tour 16, 4 Place Jussiu
75320 Paris, Cedex
France

Labor. für Festkörperphysik
ETH Hönggerberg
Attn: G. Busch
8093 Zürich
Switzerland

Labor. Festkörperphysik
ETH Hönggerberg
Attn: E. Kaldis
8093 Zurich
Switzerland

Labor. Festkörperphysik
ETH Hönggerberg
Attn: M. Piechotka
8093 Zurich
Switzerland

Labor. Festkörperphysik
ETH Hönggerberg
Attn: P. Wachter
8093 Zurich
Switzerland

Laboratoire PHASE
C. R. N.
Attn: B. Biglari
B. P. 20
F-67037 Strasbourg-Cedex
France

Laboratoire PHASE
C. R. N.
Attn: M. Hage-Ali
B. P. 20
F-67037 Strasbourg-Cedex
France

Laboratoire PHASE
C. R. N.
Attn: J. M. Koebel
B. P. 20
F-67037 Strasbourg-Cedex
France

Laboratoire PHASE
C. R. N.
Attn: M. Samimi
B. P. 20
F-67037 Strasbourg-Cedex
France

Laboratoire PHASE
C. R. N.
Attn: P. Siffert
B. P. 20
F-67037 Strasbourg-Cedex
France

Laboratoire PHASE
C. R. N.
Attn: A. Tadjine
B. P. 20
F-67037 Strasbourg-Cedex
France

LETI/CRM
CEA-CENG, 85X
Attn: M. Cuzin
38041 Grenoble, Cedex
France

LETI/CRM
CEA-CENG, 85X
Attn: Y. F. Nicolau
38041 Grenoble, Cedex
France

Link Analytical Ltd.
Attn: B. Lowe
Halifax Road, High Wycombe
Bucks, England HP12 3SE

Link Analytical Ltd.
Attn: R. Sareen
Halifax Road, High Wycombe
Bucks HP12 3SE
England

LPMC-CNRS
UA 796-UER Sciences
Attn: R. Cadoret
B. P. 45
63170 Aubière
France

Max-Planck Inst. Phys. Astroph.
Institut. für Extratr. Physik
Attn: T. Economou
c/o Dr. D. Hovestadt
8046 Garching bei München
F. R. G.

Metallurgie Hoboken Overpelt
Attn: G. Knockaert
A. Greinerstr. 14
2710 Hoboken
Belgium

NASA Headquarters
Microgravity Sci. & Appl. Div.
Code EM-7
Attn: K. Scholl
Washington, DC 20546

National Bureau of Standards
Attn: B. Steiner
Washington, DC

Office of Naval Research Branch
Division of Administration
Attn: L. Smith
223 Old Marylebone Road
London NW1 5TH
United Kingdom

Osaka University
Dept. Electrical Engineering
Faculty of Engineering
Attn: M. Suita
Osaka 565
Japan

Osaka University
Dept. Electrical Engineering
Faculty of Engineering
Attn: T. Taguchi
Osaka 565
Japan

Philips Forschungslab. GmbH
Attn: H. Scholz
Postfach 1980
D-5100 Aachen
F. R. G.

Phytoresource Research Inc.
Attn: Y. F. Abdeemessih
101E, 707 Texas Ave.
College Station, TX 77840

Radiation Monitoring Devices
Attn: G. Entine
44 Hunt St.
Watertown, MA 02172

Radiation Monitoring Devices
Attn: J. C. Lund
44 Hunt Street
Watertown, MA 02172

Robert Gordons Inst. Physics
School of Physics
Attn: J. Rennie
St. Andrews Street
Aberdeen AB1 1HG
Scotland

Robert Gordons Inst. Physics
School of Physics
Attn: M. A. S. Sweet
St. Andrews Street
Aberdeen AB1 1HG
Scotland

Schlumberger Doll Research
Attn: K.-L. Giboni
Old Quarry Road
Ridgefield, CT 06877

Scientific Industrial Automation P/L
Attn: K. J. Lieber
70 Malryborough St.
Fyshwick, ACT 2609
Australia

Scientific Industrial Automation P/L
Attn: N. F. Robertson
70 Malryborough St.
Fyshwick, ACT 2609
Australia

Scientific Industrial Automation P/L
Attn: N. Shoustov
70 Malryborough St.
Fyshwick, ACT 2609
Australia

Siemens AG Centr. Technol. Div.
Central Res. Develop., Res. Lab.
Attn: P. A. Glasow
Paul-Gossen Str. 100
D-8520 Erlangen
F. R. G.

Siemens AG Centr. Technol. Div.
Central Res. Develop., Res. Lab.
Attn: J. Walter
Paul-Gossen Str. 100
D-8520 Erlangen
F. R. G.

Techn. Büro für Kristallzücht
Ausragforschung u. Gerätebau
Attn: G. Lamprecht
Lehningerstr. 10-12
D-7531 Neuhausen
F. R. G.

Techn. Büro für Kristallzücht.
Ausragforschung u. Gerätebau
Attn: R. Lauck
Lehningerstr. 10-12
D-7531 Neuhausen
F. R. G.

Tohoku Inst. of Technology
Attn: Y. Hiratate
35-1, Yagiyama Kasulmicho
Sendai 982
Japan

Tohoku Inst. of Technology
Attn: K. Ohba
35-1, Yagiyama Kasumicho
Sendai 982
Japan

Tohoku Inst. of Technology
Attn: T. Shoji
35-1, Yagiyama Kasumicho
Sendai 982
Japan

Tokyo Denshi Yakin Co.
Attn: H. Onabe
1361 Akabane
Chigasaki-City
Kanagawa-Pref.
Japan

Toyama University
Faculty of Engineering
Attn: H. Nakatani
3190 Gofuku
Toyama 930
Japan

University of California
Dept. of Material Science Engineering
Attn: L. Keller
Los Angeles, CA 90024

University of California
Dept. Mater. Sci. Enger.
Attn: R. Ostrom
Los Angeles, CA 90024

University of California
Dept. Mat. Sci. Engineering
Attn: C. M. J. Wagner
Los Angeles, Ca 90024

University of California
Dept. Mech. Environ. Eng.
Attn: F. Milstein
Santa Barbara, CA 93106

University of California
Dept. of Physics
Attn: J. L. Merz
Santa Barbara, CA

Université Louis Pasteur
Lab. Spectr. Opt. Corps Solids
Attn: C. Schwab
5, Rue de l'Université
67084 Strasbourg, Cedex
France

Univ. Missouri-Columbia
Res. Reactor, Dept. Phys.
Attn: W. B. Yelon
Columbia, MO 65211

Univ. Southern California
Inst. Phys. Imaging Sci.
Attn: A. J. Dabrowski
4676 Admiralty Way, Suite 932
Marina del Rey, CA 90291

Univ. Southern California
Inst. Phys. Imaging Sci.
Attn: J. S. Iwanczyk
4676 Admiralty Way, Suite 932
Marina del Rey, CA 90291

Universität Bonn
Mineral. Petrogr. Inst. Museum.
Attn: F. Wollrafen
Poppelsdorfer Schloss
D-5300 Bonn
F. R. G.

Universite de Clermont II
Attn: B. Coupat
B. P. 45
63170 Aubière
France

Universite de Clermont II
Attn: J. P. Fournier
B. P. 45
63170 Aubière
France

J. H. Ewins, L-278

1000 V. Narayanamurti
1100 F. L. Vook
1110 S. T. Picraux
1112 S. M. Myers
1113 R. C. Hughes
1113 S. R. Kurtz
1113 S. J. Martin
1140 P. S. Peercy
1144 D. S. Ginley
1150 J. E. Schirber
1800 R. L. Schwoebel
4030 G. W. Kuswa
6000 D. L. Hartley
8000 J. C. Crawford
8100 E. E. Ives
8200 R. J. Detry
8300 P. L. Mattern
8310 R. W. Rohde
8340 W. Bauer
8341 M. I. Baskes
8341 R. B. James (25)
8341 G. J. Thomas
8342 M. Lapp
8343 R. H. Stulen

8343 T. E. Felter
8347 K. L. Wilson
8400 R. C. Wayne
8500 P. E. Brewer
9000 R. L. Hagengruber
9210 H. M. Dumas
9211 T. G. Taylor
9220 G. H. Mauth
9221 J. L. Williams
9222 L. S. Walker
9223 D. A. Reynolds
9224 L. J. Ellis
9230 R. E. Spalding
9231 J. C. Chavez
9232 B. C. Walker
9233 F. T. Noda
9234 W. B. Goldrick
9240 G. E. Brandvold
9241 R. L. Ewing
9241 D. J. Mitchell
9242 R. M. Hall
9243 P. B. Herrington

8535 Publication Div./ Technical
Library Processes Div., 3141

3141 Technical Library Processes
Div. (3)

8524-2 Central Technical Files (3)